M.A. KOSHELEV[1]
M.Y. TRETYAKOV[1]
R.M. LEES[2,✉]
L.-H. XU[2]

ECTDL study of N₂- and O₂-pressure broadening of a series of ammonia lines in the 1.5 µm ($v_1 + v_3$) combination band

[1] Institute of Applied Physics of Russian Academy of Sciences, 46 Uljanova Str., Nizhnii Novgorod, 603950, Russia

[2] Canadian Institute for Photonic Innovations (CIPI) and Centre for Laser, Atomic and Molecular Sciences (CLAMS), Department of Physical Sciences, University of New Brunswick, Saint John, N.B., E2L 4L5, Canada

ABSTRACT Nitrogen and oxygen pressure broadening parameters for seven $^r P(J'', 0)$ transitions of the $v_1 + v_3$ overtone band of the main isotope of ammonia with J'' varied from 2 to 9 have been measured at room temperature using an external cavity tunable diode laser spectrometer. Air-broadening parameters have also been calculated from the N_2 and O_2 measurements. The results are compared to previous measurements in the v_1, v_2, v_3, v_4 and $v_1 + v_3$ bands and to the parameters for the v_3 band that are reported in the HITRAN database.

PACS 33.70.Jg; 33.70.-W; 33.20.Ea; 42.62.Fi; 42.68.Ca

1 Introduction

Ammonia is one of the trace components of the Earth's atmosphere [1] and is also a significant species in the atmospheres of other planets, notably Jupiter [2] and Saturn [3]. Ammonia is an important pollutant gas, with atmospheric concentrations arising from agricultural, industrial and vehicle emission sources, and is also a critical trace contaminant in advanced materials manufacturing processes such as semiconductor vapor deposition and photolithography [4]. To meet the need for sensitive ammonia monitoring, a variety of diode laser techniques have been developed in recent years employing both photoacoustic detection [4–7] and direct absorption [8–14]. With the availability of good near-infrared diode sources, many of the studies have focused on absorption lines in the $v_1 + v_3$ combination and $2v_3$ overtone rovibrational bands near 1.5 µm that are the most intense and so the most appropriate for such purposes. Therefore, for reliable quantitative interpretation of the measurements, knowledge of accurate line parameters such as positions, intensities, pressure broadening and pressure shift coefficients is required for these bands.

There is a rich literature on the spectroscopy of NH_3 and on pressure broadening by a variety of collision partners. Intensity and/or line broadening studies have been carried out for a wide variety of vibrational fundamentals, combination bands and overtones as well as for the ground state in the

✉ Fax: +1-506-648-5948, E-mail: lees@unb.ca

microwave and far-infrared regions. Results are compiled in the HITRAN spectroscopic database [15] as updated in the 2000 edition [16, containing extensive references to previous work], with the line broadening data based on [17–20]. The presence of close pairs of inversion doublet lines in the NH_3 spectrum makes line mixing a significant factor and this has recently been explored in the v_4 and $2v_2$ bands for H_2 and Ar perturbers [21] and in the v_4 band for CO_2 and He [22]. For the 1.5 µm window of specific interest here for diode laser monitoring, pressure broadening measurements have been reported for several lines of the $v_1 + v_3$ band for broadening by N_2, O_2 and air [8, 23].

In our recent work [14], the line positions and absorption strengths were measured for a number of transitions of the $v_1 + v_3$ combination rovibrational band of the main isotope of ammonia using an external cavity tunable diode laser (ECTDL) spectrometer. In the present study we have continued our investigation of the $v_1 + v_3$ band line parameters and report results of room temperature N_2- and O_2-pressure-broadening measurements for the $K'' = 0$ series of NH_3 $^r P$-branch lines with quantum number J'' varied from 2 to 9, where (J'', K'') are the lower state quantum numbers of the $(J', K') \leftarrow (J'', K'')$ transition. An important feature of the $K'' = 0$ series is that it consists of single lines as opposed to close inversion doublet pairs, thus minimizing the effects of line mixing. Air-broadening parameters were calculated from the measured N_2 and O_2 parameters assuming binary collisions and a 79/21 percent atmospheric ratio of N_2 to O_2. We discuss the J-dependence of the measured broadening parameters, and compare our data to previous measurements for the v_1 [24], v_2 [20, 25, 26], v_3 [24], v_4 [19] and $v_1 + v_3$ [8, 23] bands and to the HITRAN database [15, 16].

2 Experimental details and data processing

For the present study we selected a series of relatively well isolated lines of the main ammonia isotope in the very dense $v_1 + v_3$ combination band spectrum partly covered by the operating frequency range (up to $6580 \, cm^{-1}$) of the DMD1550 laser head in our Newport 2010 ECTDL system. The series consists of $^r P$-branch ($\Delta K = +1$, $\Delta J = -1$) lines with $K = 1 \leftarrow 0$ and J'' values ranging from 2 to 9. These lines are single transitions without inversion doublet partners, contributing to the isolation. Thus in our analysis we did not

need to consider the line mixing effects that affect the shape of the inversion doublets of ammonia [21, 22, 27]. The ECTDL spectrometer described in detail in [14] was employed for the present measurements. A compact 1-m long multipass gas cell from the commercial Laser Photonics L5000 package [http://www.lasercomponents.com/] was used instead of the chamber described in [14]. To achieve maximum absorption at the minimal possible pressure of ammonia (the volume of the cell was about 13 l), we utilized 20 passes of radiation through the cell giving an absorption path length of about 20 m. For the line profile recording, the diode laser frequency was scanned by sweeping the voltage of the piezoelectric tuning element (PZT) via the GPIB interface. A Burleigh WA-1000-NIR wavemeter with a manufacturer-specified precision of ± 0.01 cm^{-1} provided readout of the laser radiation frequency. With use of the method of laser frequency calibration described in [14], we achieved a better accuracy of about ± 0.003 cm^{-1}. The laser beam passing through the multipass gas cell was detected by a New Focus Nirvana InGaAs photodiode detector operating in single channel mode. The beam was chopped at a frequency of 2.9 kHz, and synchronously detected by a Stanford Research Systems SR810 digital lock-in amplifier. The lock-in was operated in 1-f mode, and a 1-s time constant was used to obtain a sufficient signal-to-noise ratio (SNR) for accurate line parameter determination.

Each selected line was separately recorded at 8–10 different pressures of the perturbing N_2 and O_2 gases over the range from 20 to 270 Torr. At the beginning of the experiment the gas cell was filled with a small amount of ammonia and then N_2 or O_2 buffer gas was gradually added. The partial pressure of ammonia in the gas sample was varied from line to line from 0.6 to 3.1 Torr depending on the strength of the transition investigated and kept fixed during the course of the experiment on a given line. At such pressures, line half-widths did not exceed 0.04 cm^{-1} (including the Doppler half-width of about 0.01 cm^{-1}) and a 0.3–0.4 cm^{-1} scan width was chosen to be sufficient for further lineshape analysis. Each line record consisted of approximately 200 points that corresponded to a frequency step of about 0.002 cm^{-1}. To guard against possible systematic errors due to lock-in-amplifier-related lineshape distortions, both forward and backward scans were performed at each gas pressure. The two scans were analyzed separately and the line widths deduced from each fit were then averaged. We found random variations of a few percent between scan directions but no noticeable systematic differences. At each pressure, the line recording was repeated twice to obtain an estimate of the statistical errors in the line width determination.

Throughout the measurements, the absorption cell was connected to the vacuum system and the total pressure was measured with an MKS 750B Baratron gauge having a 1000 Torr full-scale reading and stated accuracy of 1%. The N_2 and O_2 gases (purity better than 99.99%) were provided by Air Liquide, Inc., and the anhydrous ammonia sample was drawn directly from a Matheson lecture bottle with purity better than 99.9%.

The experiment was carried out at room temperature as measured with a digital Micronta thermometer with 0.1 °C display resolution and 1 °C accuracy and also a standard mercury thermometer with 1 °C scale factor. Both readings coincided well and varied within the range from 21 to 25.2 °C from day to day. Daily temperature variations did not exceed 1 °C.

An empty-cell background spectrum representing the incident radiation power was recorded at the beginning $I_0^{\text{start}}(\nu)$ and at the end $I_0^{\text{end}}(\nu)$ of each set of measurements for each line studied. These two baseline records usually differed slightly from each other, hence the baseline for a measurement recorded at time t was taken as the weighted average $I_0(\nu) = (1 - C)I_0^{\text{start}}(\nu) + C I_0^{\text{end}}(\nu)$, where $C = (t - t_{\text{start}})/(t_{\text{end}} - t_{\text{start}})$.

The signal corresponding to the 0% transmission level was determined from a record of strong ammonia lines at a gas pressure sufficiently high that the line absorbed all of the radiation power. This value coincided well, to within the experimental accuracy, with the output signal observed with the detector blocked.

After accounting in this way for the spectrometer effects, we obtained the gas absorption coefficient $\alpha(\nu)$ at frequency ν from the Beer–Lambert law as

$$\alpha(\nu) \times L = \ln\left(\frac{I_0(\nu)}{I(\nu)}\right) ,$$

where $I(\nu)$ and $I_0(\nu)$ are the transmitted and the incident power, respectively, and L is the optical path length.

For further data treatment the following model function based on a Voigt line shape was fitted to the experimental profile

$$\alpha(\nu) = A_0 \int_{-\infty}^{\infty} \frac{\exp(-\tau)}{y^2 + (x - \tau)^2} \, d\tau + A_1 + A_2(\nu - \nu_0)$$
$$+ A_3(\nu - \nu_0)^2 , \qquad (1)$$

where $y = \frac{\gamma_C}{\gamma_D}\sqrt{\ln(2)}$ and $x = \frac{\nu - \nu_0}{\gamma_D}\sqrt{\ln(2)}$. Here, γ_C is the collisional line half-width at half maximum (HWHM), γ_D is the Doppler HWHM calculated for each transition as $\gamma_D = 3.581 \times 10^{-7} \nu_0 \sqrt{\frac{T}{M}}$, ν_0 is the line center frequency, T is the temperature in Kelvin and M is the molecular weight of NH_3 in atomic mass units. The A_0, A_1, A_2, A_3 are adjustable coefficients as are x, y and ν_0. The constant A_1, linear A_2 and quadratic A_3 terms are included to account for possible background variations that might arise from reflections in the spectrometer optics as well as the wings of any neighboring lines.

In a case of two or more overlapped lines lying within the record, Voigt profiles with adjustable amplitude, line center and collisional line width parameters were used for each observed line in the record and the model function was modified as

$$\alpha(\nu) = \sum_i A_0^i \int_{-\infty}^{\infty} \frac{\exp(-\tau)}{y_i^2 + (x_i - \tau)^2} \, d\tau + A_1 + A_2\nu + A_3\nu^2 ,$$
$$(2)$$

where $x_i, y_i, A_0^i, \nu_0^i, \gamma_C^i$ correspond to the parameters of (1) for the ith line. The summation extended over all blended lines in the record.

An example of the fit of the model function to the observed absorption spectrum in the vicinity of the $(s/a)^{\Delta K} \Delta J(J'', K'') = a^r P(2, 0)$ ammonia line broadened by 80.4 Torr of nitrogen

is shown in Fig. 1. (Here, the prefix s or a refers to the symmetric or antisymmetric inversion symmetry, which is conserved for transitions of the perpendicular $\nu_1 + \nu_3$ band.) The residual of the fit is presented in the lower part of the figure with the vertical scale magnified by $10\times$. The variations in the residual constitute less than 1% of the line amplitude, but do show a significant noise increase in the regions of maximum line slope where the effect of frequency fluctuations of the diode laser is enhanced. Some systematic variations also appear to be present in the fit residual that could arise from weak background NH_3 lines or could be due near the line center to small deviations from the Voigt profile arising from speed-dependent or velocity-changing effects [24] in the range of pressures when collisional and Doppler broadening are comparable. Altogether, however, the residual variations in all of our measurements did not exceed 1%–2%. It was demonstrated in [24] that under these conditions, the use of more elaborate line profiles that account for speed dependence or Dicke line narrowing leads to less than 1% deviation from the line broadening parameter determined from a Voigt profile, supporting our choice of this simpler model.

3   Results and discussion

Our experimental collisional linewidths γ_C for the $a^r P(6, 0)$ ammonia transition are plotted in Fig. 2 as a function of the total pressure of the gas mixture for nitrogen (filled diamonds) and oxygen (open circles) perturbing gases. Each point corresponds to the averaged line half-width for forward and backward scans. The pressure-broadening parameters were determined as the slope of a linear function fitted to the experimental points. The residuals of the fits to both N_2- and O_2-broadening data for the $a^r P(6, 0)$ transition are shown in the lower part of Fig. 2, using the same symbols as for the corresponding experimental points, with 1-σ error bars in the experimental half-widths. Self-broadening was considered to be minimal for the small partial pressures of ammonia employed, and would not affect the slopes of the fitted lines since the pressure of ammonia in the cell was fixed. The linear
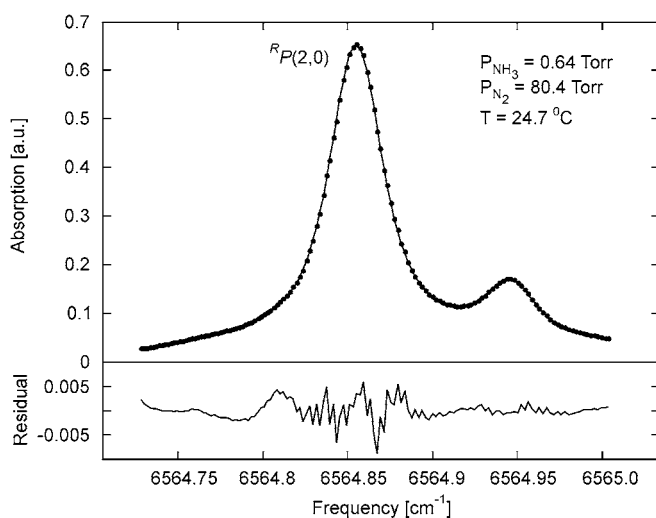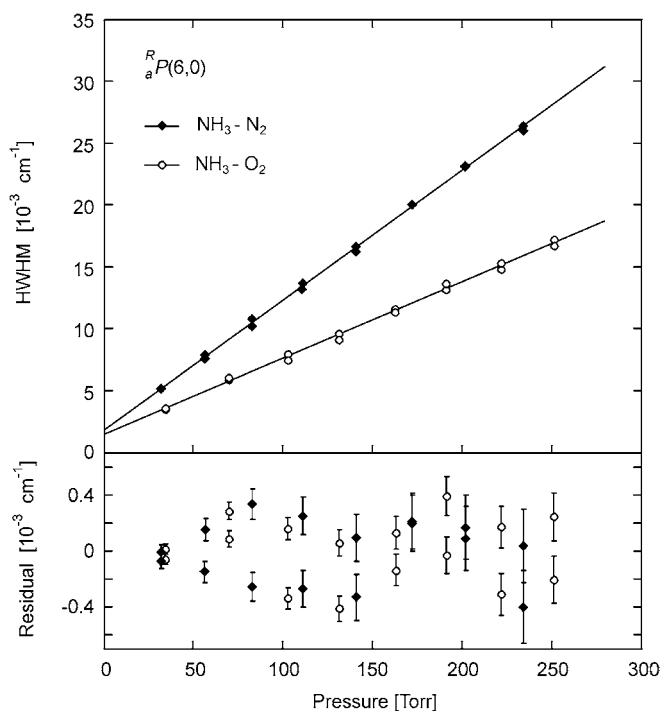

FIGURE 2   Dependence of the line width (HWHM) vs. total pressure in the cell for the $a^r P(6, 0)$ ammonia line broadened by nitrogen (filled diamonds) and oxygen (open circles). Residuals of the linear regression (solid lines passing through the experimental points) are shown underneath with error bars corresponding to 1-σ statistical uncertainties in measured half-widths

fits accurately represent the data down to the lowest pressures studied with no evidence of systematic deviations in the residuals.

The values of the N_2- and O_2-pressure-broadening parameters γ^{N_2} and γ^{O_2} determined in the present study are listed in Table 1, together with the air-broadening parameters γ^{Air} calculated as

$$\gamma^{Air} = 0.79\gamma^{N_2} + 0.21\gamma^{O_2}. \tag{3}$$

Since the data were obtained at slightly different temperatures over the range 21–25.2 °C, all values were normalized to a universal temperature of 24 °C employing the commonly used formula $\gamma_C(T_0) = \gamma_C(T)(T/T_0)^n$ for the temperature-dependence of the broadening with an exponent of $n = 0.8$ taken from the Institute of Atmospheric Optics database [http://spectra.iao.ru] and consistent with the experimental results of [28]. A variation of n within the range 0.6 to 1.0 (the limits from [28] for various ammonia lines) would lead to less than 0.2% change of broadening parameter. Since the normalization of the broadening to the standard 24 °C also corresponded to a change of 0.15%–0.25%, the total error arising from the data temperature correction does not exceed 0.5% as a conservative estimate.

In general, we believe that the 3-σ uncertainties given in Table 1, corresponding to 2%–8% of the broadening parameter values, are realistic estimates of the actual experimental errors including all possible systematic deviations.

Figure 3 shows our experimental broadening parameters (filled circles) plotted as a function of rotational quantum number J'' and compares them to previous measurements

FIGURE 1   Model function (solid line) fitted to the experimental record (points) of the $(s/a)^{\Delta K} \Delta J(J'', K'') = a^r P(2, 0)$ ammonia line broadened by 80.4 Torr of nitrogen. The residual of the fit is presented below

Transition $(s/a)^{\Delta K}$ $\Delta J(J'', K'')$	Wavenumber[a] [cm^{-1}]	Pressure-broadening parameter γ (in cm^{-1} atm^{-1})[b] NH$_3$–N$_2$	NH$_3$–O$_2$	NH$_3$–air
a$^r P$(2,0)	6564.85	0.1126(30)	0.0711(27)	0.1039(30)
s$^r P$(3,0)	6544.31	0.1007(27)	0.0606(18)	0.0923(25)
a$^r P$(4,0)	6525.12	0.0910(21)	0.0527(30)	0.0830(23)
a$^r P$(6,0)	6482.69	0.0799(18)	0.0462(21)	0.0728(19)
s$^r P$(7,0)	6464.39	0.0732(18)	0.0435(18)	0.0670(18)
a$^r P$(8,0)	6443.45	0.0646(27)	0.0401(30)	0.0595(28)
s$^r P$(9,0)	6422.43	0.0578(21)	0.0377(30)	0.0536(23)

TABLE 1   Experimental pressure-broadening parameters for NH$_3$ at 24 °C

[a] Wavenumbers are taken from [14]
[b] Errors in parentheses correspond to three standard deviation uncertainties (3-σ) in the last digit
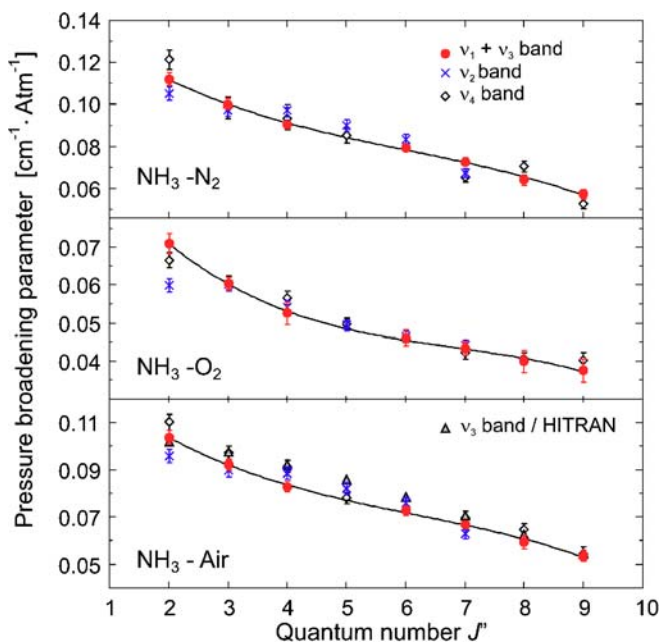

FIGURE 3   Measured N$_2$-, O$_2$- and calculated air-pressure-broadening parameters for the $^r P(J'', 0)$ transitions of ammonia, presented as a function of J'' in *upper*, *middle* and *lower figures*, respectively. Our values are shown by *filled circles* while those for the ν_2 [20] and ν_4 band [19] are plotted as *crosses* and *open diamonds*, respectively. The ν_3 band HITRAN data [15, 16] for air-broadening are shown by *triangles*. The *solid lines* represent third-order polynomial interpolations of our data

$\lvert m \rvert$	Perturber	Previous studies γ (cm^{-1} atm^{-1})	Band	Present study $\nu_1 + \nu_3$ band[a]
1	N$_2$	0.11345(9)	ν_1 [24]	0.1282
	O$_2$	0.06341(6)		0.0860
	N$_2$	0.1129	ν_2 [20]	
	O$_2$	0.0641		
	N$_2$	0.1146	ν_2 [25, 26]	
	O$_2$	0.0660		
2	N$_2$	0.10641(4)	ν_1 [24]	0.1126(30)
	O$_2$	0.06069(3)		0.0711(27)
	N$_2$	0.1056	ν_2 [20]	
	O$_2$	0.0601		
	O$_2$	0.0667(20)	ν_4 [19]	
3	N$_2$	0.0978	ν_2 [20]	0.1007(27)
	O$_2$	0.0604		0.0606(18)
	N$_2$	0.0989(51)	ν_4 [19]	
	O$_2$	0.0608(18)		
4	N$_2$	0.09697(4)	ν_1 [24]	0.0910(21)
	O$_2$	0.05511(3)		0.0527(30)
	N$_2$	0.0977	ν_2 [20]	
	O$_2$	0.0544		
	N$_2$	0.0938(51)	ν_4 [19]	
	O$_2$	0.0568(18)		
5	N$_2$	0.0906	ν_2 [20]	0.0849
	O$_2$	0.0496		0.0488
	N$_2$	0.0921(8)	ν_3 [24]	
	O$_2$	0.0524(4)		
	O$_2$	0.0499(15)	ν_4 [19]	
6	N$_2$	0.0838	ν_2 [20]	0.0799(18)
	O$_2$	0.0465		0.0462(21)
	N$_2$	0.0785(40)	$\nu_1 + \nu_3$ [8]	
7	N$_2$	0.0679	ν_2 [20]	0.0732(18)
	O$_2$	0.0404		0.0435(18)
	N$_2$	0.0659(25)	ν_4 [19]	
	O$_2$	0.0423(18)		
8	N$_2$	0.0710(25)	ν_4 [19]	0.0646(27)
	O$_2$	0.0408(15)		0.0401(30)
9	N$_2$	0.0547	ν_2 [20]	0.0578(21)
	O$_2$	0.0392		0.0377(30)
	N$_2$	0.0532(25)	ν_4 [19]	
	O$_2$	0.0403(20)		

[a] Parameters for transitions with $\lvert m \rvert = 1$ and 5 were not measured in the present study but were determined from the third-order polynomial regression to our experimental data

TABLE 2   Comparison of N$_2$- and O$_2$-pressure-broadening parameters for $K'' = 0$ transitions of different rovibrational bands of NH$_3$

for analogous $K'' = 0$ P-branch transitions in the ν_2 [20] and ν_4 [19] bands as well as the HITRAN values for air-broadening [15, 16]. Note that for some of our data points, the small 3-σ error bars are hidden inside the points. A strong variation of about 50% is seen for the pressure broadening parameter over the range of J'' studied in the present work. As a polynomial approximation to the variation of line broadening with J and K is quite common (see e.g. [20] and references therein), we approximated the dependence on J by third-order polynomials (shown in Fig. 3 as solid lines) in order to demonstrate the smoothness and the monotonic trends of the derived broadening parameters. Deviations of the experimental points from the polynomial curves do not exceed 50% of the estimated experimental uncertainty for N$_2$-broadening and 30% for the O$_2$-broadening data. Our observed ratio $\gamma^{N_2}/\gamma^{O_2}$ between the nitrogen and oxygen broadening parameters is about 1.6, comparable to the factor of about 1.8 for observations reported previously [23] for a different set of $\nu_1 + \nu_3$ transitions at higher wavenumber with $K'' > 0$.

Comparison of our data with those shown in Fig. 3 for the P-branches of the ν_2 [20] and ν_4 [19] bands demonstrates good general agreement with small statistical deviations within 7%–8% that are only slightly in excess of the estimated uncertainties. A somewhat more regular discrepancy in the air-broadening parameters is seen between our

values and those taken from the HITRAN database for the ν_3 band [15, 16], shown by triangles.

To further place our results in context against those reported previously for different bands of NH_3, we summarize in Table 2 the values of N_2- and O_2-broadening parameters for $K'' = 0$ transitions as a function of $|m|$ ($m = -J$ for P-branch and $m = J + 1$ for R-branch). Broadening parameters for transitions with $|m| = 1$ and 5 were not measured in the present study, hence we list instead the calculated values from our third-order polynomial regressions. Table 2 shows general consistency among the broadening parameters for the different vibrational bands over the whole range of $|m|$ studied, with no evidence of systematic differences between the bands. For $|m| = 1$, the discrepancies in our broadening coefficients are somewhat larger, possibly associated with the uncertainty in the polynomial extrapolation of our data. (Note that since we did not aim towards modification of the empirical expressions for the pressure broadening rotational dependence [17, 20] and used a polynomial here primarily to demonstrate the smoothness of our data, our polynomial coefficients are not presented. For detailed analysis of the rotational dependence of the broadening upon J, we recommend use of the original experimental values shown in Table 1.)

4   Conclusion

The nitrogen and oxygen pressure-broadening coefficients of a series of seven ^rP transitions from the $\nu_1 + \nu_3$ band of $^{14}NH_3$ with $K'' = 0$ and J'' varied from 2 to 9 have been measured at room temperature using an ECTDL spectrometer. The corresponding coefficients for air-broadening were calculated from the measured N_2 and O_2 values. The O_2 broadening coefficients are found to be systematically smaller than those for N_2 by a factor of about 1.6. A significant decrease of the pressure broadening parameters with increasing J'' is observed for the $\nu_1 + \nu_3$ band, as expected. The experimental results obtained are in good general agreement with those measured by other authors for the same band as well as for other vibrational bands, and there do not appear to be any systematic differences among the vibrational states. Comparison with HITRAN data for the ν_3 band also indicates a closely similar trend with J'' but with somewhat lower values for the pressure-broadening parameters. In general, our results suggest that existing database information for other vibrational bands of ammonia may be extended with some confidence to the $\nu_1 + \nu_3$ band of NH_3 with its important applications for TDL atmospheric sensing and industrial process monitoring. In future, with the acquisition of diode lasers at higher wavenumber to cover the Q and R branch regions of the $\nu_1 + \nu_3$ band, we would like to test this conclusion further by extending the study and including transitions of higher K in order to explore both the K- and J-dependence of the collisional broadening over a broad manifold of rotational states.

REFERENCES

1 V. Ramanathan, R.J. Cicerone, H.B. Singh, J.T. Kiehl, J. Geophys. Res. **90**, 5547 (1985)

2 V. Kunde, R. Hanel, W. Maguire, J.P. Baluteau, A. Marten, A. Chedin, H. Housson, N.S. Scott, Astrophys. J. **263**, 443 (1982)

3 P.T.P. Ho, C.H. Townes, Ann. Rev. Astron. Astrophys. **21**, 239 (1983)

4 S. Schilt, L. Thevenaz, M. Nikles, L. Emmenegger, C. Huglin, Spectrochim. Acta A **60**, 3259 (2004)

5 Z. Bozoki, A. Mohacsi, G. Szabo, Z. Bor, M. Erdelyi, W. Chen, F.K. Tittel, Appl. Spectrosc. **56**, 715 (2002)

6 V. Horka, S. Civis, L.-H. Xu, R.M. Lees, Analyst **130**, 1148 (2005)

7 M. Mattiello, M. Nikles, S. Schilt, L. Thevenaz, A. Salhi, D. Barat, A. Vicet, Y. Rouillard, R. Werner, J. Koeth, Spectrochim. Acta A **63**, 952 (2006)

8 G. Modugno, C. Corsi, Infrared Phys. Technol. **40**, 93 (1999)

9 R. Peeters, G. Berden, A. Apituley, G. Meijer, Appl. Phys. B **71**, 231 (2000)

10 M.E. Webber, D.S. Baer, R.K. Hanson, Appl. Opt. **40**, 2031 (2001)

11 R. Claps, F.V. Englich, D.P. Leleux, D. Richter, F.K. Tittel, R.F. Curl, Appl. Opt. **40**, 4387 (2001)

12 Z. Bozoki, A. Mohacsi, G. Szabo, Z. Bor, M. Erdelyi, W. Chen, F.K. Tittel, Appl. Spectrosc. **56**, 715 (2002)

13 G. Totschnig, M. Lackner, R. Shau, M. Ortsiefer, J. Rosskopf, M.C. Amann, F. Winter, Appl. Phys. B **76**, 603 (2003)

14 L.-H. Xu, Z. Liu, I. Yakovlev, M.Yu. Tretyakov, R.M. Lees, Infrared Phys. Technol. **45**, 31 (2004)

15 L.S. Rothman, D. Jacquemart, A. Barbe, D.C. Benner, M. Birk, L.R. Brown, M.R. Carleer, C. Chakerian Jr., K. Chance, V. Dana, V.M. Devi, J.-M. Flaud, R.R. Gamache, A. Goldman, J.-M. Hartmann, K.W. Jucks, A.G. Maki, J.-Y. Mandin, S.T. Massie, J. Orphal, A. Perrin, C.P. Rinsland, M.A.H. Smith, J. Tennyson, R.N. Tolchenov, R.A. Toth, J. Vander Auwera, P. Varanasi, G. Wagner, J. Quantum Spectrosc. Radiat. Transf. **96**, 139 (2005)

16 I. Kleiner, G. Tarrago, C. Cottaz, L. Sagui, L.R. Brown, R.L. Poynter, H.M. Pickett, P. Chen, J.C. Pearson, R.L. Sams, G.A. Blake, S. Matsuura, V. Nemtchinov, P. Varanasi, L. Fusina, G. Di Lonardo, J. Quantum Spectrosc. Radiat. Transf. **82**, 293 (2003)

17 L.R. Brown, D.B. Peterson, J. Mol. Spectrosc. **168**, 593 (1994)

18 V.N. Markov, A.S. Pine, G. Buffa, O. Tarrini, J. Quantum Spectrosc. Radiat. Transf. **50**, 167 (1993)

19 H. Aroui, M. Broquier, A. Picard-Bersellini, J.P. Bouanich, M. Chevalier, S. Gherissi, J. Quantum Spectrosc. Radiat. Transf. **60**, 1011 (1998)

20 V. Nemtchinov, K. Sung, P. Varanasi, J. Quantum Spectrosc. Radiat. Transf. **83**, 243 (2004)

21 M. Dhib, M.A. Echargui, H. Aroui, J. Orphal, J.-M. Hartmann, J. Mol. Spectrosc. **233**, 138 (2005)

22 M. Dhib, M.A. Echargui, H. Aroui, J. Orphal, J. Mol. Spectrosc., unpublished, DOI: 10.1016/j.jms.2006.04.013

23 J.S. Gibb, G. Hancock, R. Peverall, G.A.D. Ritchie, L.J. Russell, Eur. Phys. J. D **28**, 59 (2004)

24 A.S. Pine, V.N. Markov, J. Mol. Spectrosc. **228**, 121 (2004)

25 M. Fabian, F. Ito, K.M.T. Yamada, J. Mol. Spectrosc. **173**, 591 (1995)

26 M. Fabian, F. Ito, K.M.T. Yamada, J. Mol. Spectrosc. **236**, 150 (2006)

27 S. Hadded, H. Aroui, J. Orphal, J.-P. Bouanich, J.-M. Hartmann, J. Mol. Spectrosc. **210**, 275 (2001)

28 S. Nouri, J. Orphal, H. Aroui, J.-M. Hartmann, J. Mol. Spectrosc. **227**, 60 (2004)